Simulation of Radiation Shielding and Elastic Moduli Properties of Gd^{3+} on Ce^{3+}/Tb^{3+} Co-Doped some Scintillating Glasses

Kittisak Sriwongsa[a,b,] *, Sunantasak Ravangvong[c], Chumphon Khobkham[d], Punsak Glumglomchit[e], Nutwara Uammuang[e], Kotchamon Thammachot[e], Priyakorn Chaiyo[e]

[a]*Lecturers responsible for Bachelor of Education Program in Physics, Faculty of Education, Silpakorn University, Nakhon Pathom, 73000 Thailand*
[b]*The demonstration school of Silpakorn University, Nakhon Pathom, 73000 Thailand*
[c]*Division of Science and Technology, Faculty of Science and Technilogy, Phetchaburi Rajabhat University, Phetchaburi, 76000 Thailand*
[d]*Faculty of Engineering, Thonburi University, Bangkok, 10160 Thailand*
[e]*Huahin Vitthayalai School, Hua–Hin, Prachuap Khiri Khan, 77110 Thailand*

Received 9 July 2019; Revised 6 November 2019; Accepted 13 December 2019

Abstract

The aim of this research is to study the radiation shielding and elastic moduli of Gd^{3+} on Ce^{3+}/Tb^{3+} co-doped some scintillating glasses. The mass attenuation coefficients (μ_m), of scintillating glasses have also been computed in the energy range 1 keV – 100 GeV using WinXCOM software program. The effective atomic number (Z_{eff}), effective electron density (N_{el}) and half value layer (*HVL*) have been computed. The lower values of *HVL* indicate that the scintillating glasses possess better shielding properties. The oxygen packing density (*OPD*), molar volume (V_m), number of bonds per unit volume, average cross-link density and packing density have also been obtained. The modulus of elasticity for samples are calculated by Makishima and Mackenzie mode and compared among themselves. The GTC15 scintillating glass has highest value of elastic modulus.

KEYWORDS: scintillating glass; radiation shielding properties; elastic moduli

*Corresponding authors ; E-mail : sriwongsa_k@silpakorn.edu

Introduction

Recently, glass scintillator is favors used in many fields such as medical, well-logging, nuclear facilities, security, X-ray detection and high energy physics. The demand of glass scintillating glass as high density and high luminous intensity were increased which the high density of scintillating glass can be done by doped rare-earth ions. The doping rare-earth ions were caused the energy transfer between rare earth ions and activation ions which made luminous were high intensity. The rare-earth doped scintillating glass was wildly used because of its large-volume production, low cost and creating elements easily compared with scintillating crystals or ceramics. The rare earth doped glass material had properties in good quickness for emitting visible and absorbing UV-visible radiations which may make it had tended to be used as for electromagnetic radiations detection. Therefore, the applied utility of rare earth doped glass materials was interested used for high energy radiation shield sensing and designing [1 – 4].

Among all heavy rare earth ions, Gadolinium (Gd^{3+}) is interested element due to it can applied in several field such as gamma and neutron detectors and shielding nuclear reactors. Gadolinium had high density (7.895 g cm^{-3}), did not produce color center glass, high stopping power with a melting point of 1313 °C and high atomic number (Z = 64) so the probability of interaction of gamma rays with it is very high [5 – 7].

In this context, Gd^{3+} on Ce^{3+}/Tb^{3+} co-doped Gd_2O_3-B_2O_3-SiO_2 (GBS) scintillating glasses are to simulate on radiation shielding properties such as mass attenuation coefficient (μ_m), effective atomic number (Z_{eff}), electron density (N_{el}) and half value layer in energy range 1 keV – 100 GeV by WinXCOM software program and their elastic moduli were calculated using Makishima-Mackenzie (M-M) model.

Materials and Methods

The theoretical/method basis have been separated into following sub-sections:

Radiation shielding parameters

The theoretical computation of mass attenuation coefficients for scintillating glasses using WinXCom software program for photon at energies range 1 keV – 100 GeV by Eq. (1) [8 – 9]:

$$\mu_m = \sum_i^n W_i\left(\mu_m\right) \quad (1)$$

where W_i and μ_m are weight fraction and mass attenuation coefficient of element *i*, respectively. The effective atomic numbers for glasses series can be determined from Eq. (2) [8 – 9]:

$$\sigma_{t,a} = \frac{\mu_m M}{N_A \sum_i n_i} \quad (3)$$

$$\sigma_{e,ei} = \frac{1}{N_A}\sum_i \frac{f_i}{Z_i} A_i (\mu_m)_i \quad (4)$$

where M, n_i, N_A, f_i, Z_i and A_i are molecular weight of mixture component in scintillating glasses, number of oxygen atoms per each composition, Avogadro's number, respectively.

The electron densities (N_{el}) for scintillating glasses refer to number of electron per unit mass can be computed by formula from Eq. (5) [8 – 9]:

$$N_{el} = \frac{\mu m}{\sigma_{t,el}} \quad (5)$$

The half value layer is quantity describing thickness of attenuator that attenuation of photon density to half of incident energy as the lower of *HVL* value is better shielding effectiveness and can be calculated using by Eq. (6) [8, 11 – 12]:

$$HVL = \frac{0.693}{\mu} \quad (6)$$

Where μ is linear attenuation coefficient.

Physical and elastic parameters

The molar volume has been determined by formula relation in Eq. (7) [8]:

$$V_m\left(cm^3/mol\right) = \frac{M}{\rho} \quad (7)$$

Where M and ρ are molecular weight and density of mixture component in scintillating glasses. Oxygen molar volume (V_0) has been used formula to estimate by Eq. (8) [8]:

$$V_0 = V_m\left(\frac{1}{\sum x_i n_i}\right) \quad (8)$$

The next, oxygen packing density can be determined by following Eq. (9) [8]:

$$OPD = 1000N\left(\frac{\rho}{M}\right) \quad (9)$$

Where X_i, M_i, n_i and N are molar fraction of i-th component, molecular weight of i-th, number of oxygen atoms in each constituent oxide and number of oxygen atoms per each composition, respectively. The average cross-link density ($\bar{n}_c$) the number of bonds per unit volume values (n_b) of scintillating glasses can be computed using following Eq. (10) [8]:

$$\bar{n}_c = \frac{\sum x_i (n_c)_i (N_c)_i}{\sum x_i (N_c)_i} \quad (10)$$

$$n_b = \frac{N_A}{V_m}\sum (n_f)_i x_i \quad (11)$$

where n_c, N_c, N_A and n_f are crosslink per cations, number of cations per glass formula unit, Avogadro's number and coordination number of the cations of each component oxide and *i* represents component oxide. Maskishima and Mackenzie were calculated elastic modulus of oxide glasses by theoretically model (M–M model) based on chemical component, packing density (V_t) and dissociation energy per unit volume (G_t) of glasses as following by Eq. (12) [8, 10]:

Packing density (V_t): $$V_t = \left(\frac{1}{V_m}\right)\sum V_i x_i \quad (12)$$

Where, $Vi = NA\left(\frac{4\pi}{3}\right)\left(xR_A^3 + yR_O^3\right)$, R_A and R_O are ionic radius of metal and oxygen, respectively. Young's (E), shear (G), longitudinal (L) modulus, Poisson's ratio (σ), fractal bond connectivity (d), and hardness (H) and bulk (K)

have been calculated as following by Eq. (13 – 19)

Young's modulus (E): $E = 8.36 V_t G_t$ (13)

Shear modulus (G): $G = \frac{30 V_t^2 G_t}{(10.2 V_t - 1)}$ (14)

Longitudinal modulus (L): $L = K + \left(\frac{4}{3}\right) G$ (15)

Poisson's ration (σ): $\sigma = 0.5 - \left(\frac{1}{7.2 V_t}\right)$ (16)

Fractal bond connectivity (d): $d = 4\left(\frac{G}{K}\right)$ (17)

Hardness (H): $H = \frac{(1-2\sigma)E}{6(1+\sigma)}$ (18)

Bulk (K): $K = 10 V_t^2 G_t$ (19)

The chemical compositions of the scintillating glasses have been shown in Table 1.

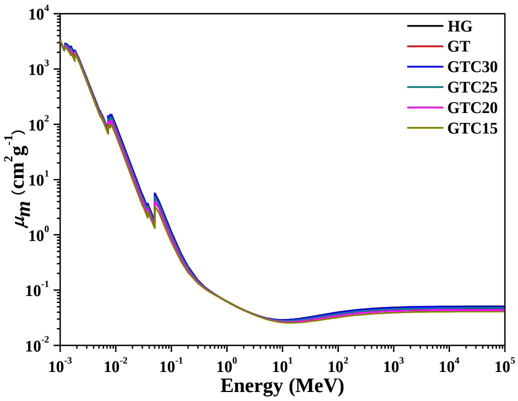

Fig. 1 μ_m of scintillating glasses calculated at energy 1 keV – 100 GeV.

The mass attenuation coefficients

The μ_m of the scintillating glasses have been computed using WinXCom software program at energy range 1 keV – 100 GeV energies as shown in Fig. 1. It is also clear that,

Table 1 The chemical compositions of scintillating glasses in wt. fraction of elements [1].

Code	Wt. fraction of elements									
	Si	B	Ba	Al	Gd	P	Tb	Ce	Sb	O
GTC30	0.12	0.07	0.03	0.05	0.26	0.01	0.04	0.002	0.004	0.41
GTC25	0.14	0.07	0.03	0.05	0.22	0.01	0.04	0.002	0.004	0.43
GTC20	0.16	0.07	0.03	0.05	0.17	0.01	0.04	0.0012	0.004	0.45
GTC15	0.19	0.07	0.03	0.05	0.13	0.01	0.04	0.002	0.004	0.47

Table 2 The photon energies (in × 10^{-3} MeV) of absorption edges for elements.

Element	M5	M4	M3	M2	M1	L3	L2	L1	K
Si	–	–	–	–	–	–	–	–	1.84
Al	–	–	–	–	–	–	–	–	1.56
P	–	–	–	–	–	–	–	–	2.14
Sb	–	–	–	–	–	4.13	4.38	4.7	30.49
Ba	–	–	1.06	1.14	1.29	5.25	5.62	5.99	37.44
Ce	–	–	1.18	1.27	1.44	5.72	6.16	6.55	40.44
Gd	1.18	1.22	1.54	1.69	1.88	7.24	7.93	.376	50.24
Tb	1.24	1.27	1.61	1.77	1.97	7.51	8.25	8.71	52.00

Results and Discussion

Radiation shielding parameters

the variant of μ_m value depend on the energy and the composition of the measured scintillating glasses. The main interaction of photon: Photoelectric absorption, Compton Scattering (incoherent) and Pair Production can be illustrated the interaction of photons with oxide scintillating glasses. Low energy (energy is less than 0.1 MeV), the μ_m trend of scintillating glasses deceases very quickly with increasing photon energy, and the μ_m value peak were discontinuities because of absorption edge of element as shown in table 2. The rapid reduction in μ_m at E < 0.3 MeV may be caused by that cross section of photoelectric effect is conversely relative to photon energy ($E^{3.5}$). Intermediate energy (energy is less than 10 MeV and is greater than 0.3 MeV), the values of μ_m decrease at slower with increment of photon energy. This might be the Compton Scattering (incoherent) process becomes the main mechanism, and this was because of the cross section of Compton Scattering is conversely relative to photon energy (E^{-1}) and it changes linearly with nuclear number Z. High energy (energy is greater than 10 MeV), the μ_m values increase nearly constant. In this energy range, the pair production process starts dominant interaction whose cross section depends on atomic number (Z^2). It is noticed that μ_m values increase with increment in Gd_2O_3 concentration in scintillating glasses. This is because of the lowest weight fraction of Gd_2O_3 in GTC15 scintillating glass and increases in weight fraction of Gd_2O_3 in the continuous scintillating glasses which results in increase in μ_m values, so, the GTC30 scintillating glass is a better gamma ray shielding scintillating glass.

Effective atomic numbers and electron densities

The calculation of Z_{eff} and N_{el} value with photon energy for scintillating glasses has been shown in Fig. 2 and Fig. 3, respectively. Clearly, the Z_{eff} values for scintillating glasses are found to increase with increase in Gd_2O_3 concentrations as shown in Fig. 2. The increase in Z_{eff} is referring to replacement of SiO_2 by Gd_2O_3 which have a higher effective atomic cross-section than SiO_2. In term of photon energy, the Z_{eff} value for scintillating glasses increases with increment of photon energy and shifts happen at 1.5 keV, 20 keV and 60 keV. These shifts can be discussed on k edge absorption. The Z_{eff} values of scintillating glasses in energy range 1 – 20 keV, are nearly independent of photon energy. Thereafter, energy from 60 – 300 keV, Z_{eff} value rapidly decrease with increasing energy for all scintillating glasses; this can be discussed on basic of the dependence of cross-section of photoelectric absorption which changes inversely with photon energy as $E^{3.5}$. After that, increase of photon energy in range 0.3 – 10 MeV, Z_{eff} value for all scintillating glasses becomes nearly independent of photon energy. This may be because of major of Compton scattering (incoherent) process. As photon energy increases above 10 MeV, Z_{eff} value slowly increases and becomes nearly constant above 100.0 MeV. This can be discussed based on the major of pair production in this higher energy range. The electron density with photon energy in the range 1 keV – 100 GeV as shown in Fig. 3, has demonstrated the same behavior of Z_{eff}.

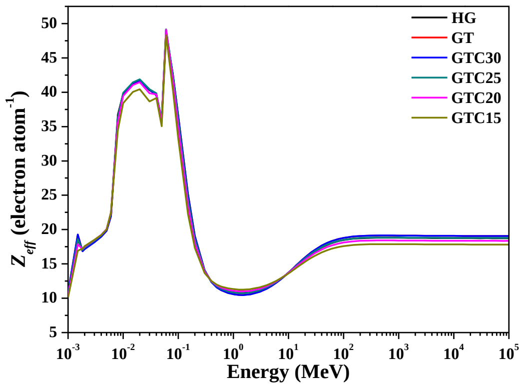

Fig. 2 Z_{eff} of scintillating glasses calculated at energy 1 keV–100 GeV.

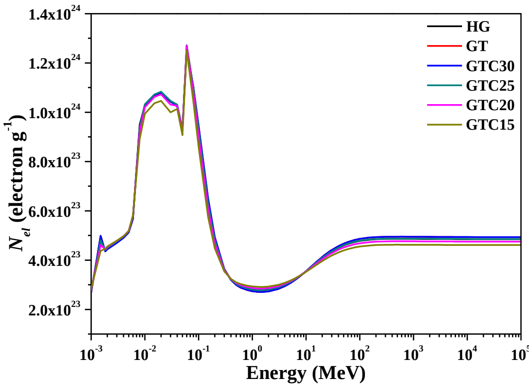

Fig. 3 N_{el} of scintillating glasses calculated at energy 1 keV – 100 GeV.

The half value layer is one of quantities explaining radiation attenuation which lower *HVL* values is a better radiation shielding material. The relation of *HVL* with photon energy was shown in Fig. 4. Clearly, *HVL* values were almost constant up to 0.1 MeV and gradually increased in energy up to 10 MeV. For photon energy > 10 MeV, *HVL* values show decrease with increasing photon energy and becomes nearly constant above 10^3 MeV. This differentiation is accepted in terms of dependency in cross section values on energy for different major photon interaction processes in variance energy range. In lower energy range, cross-section of photoelectric absorption is found in the inverse proportionality with energy as $E^{-3.5}$. It means that the more reduce energy, the probability of interaction between photon and medium via photoelectric absorption will be higher and then the thickness is less than enough to absorb photons in the medium being examined. On the other hand, the increment in thickness of interacting medium is necessary for interaction of photon. *HVL* values rise gradually for scintillating glasses that because of this strong confidence in cross–section of energy. In the intermediate energy range, cross-section for Compton scattering (incoherent) is found in linear relation with photon energy. *HVL* values increase with slow rates for the selected scintillating glasses that due to this weak confident in cross-section of energy. Cross–section for pair production shows logarithmic differentiation with energy in high range. Thus, in high photon energy, the probability of interaction between photon and medium via pair production tends to happen in exponential nature. Therefore, the thickness requirement may decrease when photon energy is high for better absorption in medium. In these results, GTC 30 has lowest *HVL* value so it is the best radiation shielding scintillating glasses.

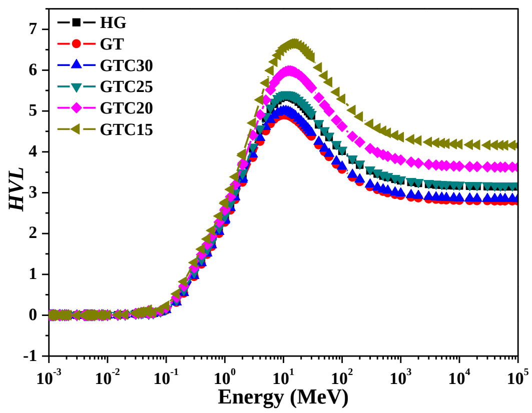

Fig. 4 *HVL* of scintillating glasses calculated at energy 1 keV – 100 GeV.

Physical and elastic parameters

The oxygen packing density, molar volume, oxygen molar volume (V_0), number of bonds per unit volume (n_b) and average cross-link density ($\bar{n}_c$) of scintillating glasses are given in Table 3. The values of *OPD*, V_0 and n_b decrease while V_m and $\bar{n}_c$ increase with increasing Gd_2O_3 concentration. The behavior of V_m may be caused by the ionic radius of Gd (0.94 Å) is bigger than the ionic radius of Si (0.40 Å) and create non-bridging oxygens. The modifier ions (Gd) catch with oxygen ions occur the large size and molar volume. The decrease in *OPD* indicates that the scintillating glasses structure had more loosely bound. Oxygen molar volume values showed decrease with increased Gd_2O_3 content as the scintillating glasses structure had more density. The increase in average cross-link density with increasing Gd_2O_3 concentration indicates that network of scintillating glasses had more connected and increase the number of bridging oxygen atoms; so, the average cross-link density increases.

The computed values of packing density (V_t), Young's (E), bulk (K), shear (G), longitudinal (L) modulus, Poisson's ratio (σ), fractal bond connectivity (d) and hardness (H) using Makishima and Mackenzie (M-M) model for scintillating glasses have been listed in Table 4. The fractal bond connectivity (d) is a helpful parameter implicated the mechanical properties of scintillating glasses to their formations. This parameter is the data about the effective dimensionality and crosslinks of scintillating glasses network. The d is 1, 2 and 3 for the chain, layer formation and 3D networks of tetrahedral coordination polyhedral. From Tables 4 the d values of computing scintillating glasses were increase with increasing G_2O_3 content. These values closed to 2 which mean that the scintillating glasses network has 2D layer formation.

Poisson's ratio (σ) values decrease with increasing Gd_2O_3 concentration. The σ values indicate the formation bonds of scintillating glasses become loosing and so the decrease in scintillating glasses formation rigidity. As shown in Tables 4 the computed elastic modulus (E, L, K, and G) for to scintillating glasses decrease with increasing Gd_2O_3 concentration. It is clear that, the GTC15 scintillating glass sample has the highest elastic modulus.

Table 3 Density , oxygen packing density, molar volume, oxygen molar volume, number of bonds per unit volume and average cross-link density of scintillating glasses.

Code	ρ (g cm^{-3})	*OPD* (mol L^{-1})	V_m (g mol^{-1})	V_0 (cm^3 mol^{-1})	$n_b \times 10^{23}$ (cm^{-3})	$\bar{n}_c$
GTC30	4.80	89.00	30.86	0.09	9.76	3.01
GTC25	4.59	95.38	28.28	0.09	1.04	2.98
GTC20	4.31	102.09	25.93	0.10	1.11	2.82
GTC15	4.05	112.27	23.13	0.11	1.22	2.72

Table 4 Packing density (V_t), Young's (E), bulk (K), shear (G), longitudinal (L) modulus, Poisson's ratio (σ), fractal bond connectivity (d) and hardness (H) of scintillating glasses.

Code	V_t	E (GPa)	K, (GPa)	G (GPa)	L (GPa)	σ	d	H (GPa)
GTC30	0.67	31.32	25.25	12.89	42.44	0.29	2.04	2.043
GTC25	0.72	34.77	29.79	14.17	48.69	0.31	1.90	1.903
GTC20	0.76	38.46	34.98	15.53	55.69	0.32	1.78	1.78
GTC15	0.83	43.62	43.23	17.40	66.44	0.33	1.61	1.61

Conclusion

In this work, the μ_m, Z_{eff}, N_{el} and *HVL* of scintillating glasses have been simulated in energy range 1 keV – 100 GeV. The GTC30 scintillating glass was found that μ_m was decreased with increasing energy because of the dominance of photoelectric absorption, Compton scattering and pair production in selected energy range. The *HVL* for GTC30 scintillating glass sample was least that indicated it is the best shielding scintillating glasses. The decrease in *OPD* indicates that the scintillating glasses formation is loosely bound. The fractal band connectivity (d) values for these scintillating glasses present that the scintillating glasses network have 2-D layer formation. The GTC15 has the highest value of elastic modulus.

Acknowledgement

The authors wish to acknowledge the instrument support from Center of Excellence in Glass Technology and Materials Science (CEGM), Nakhon Pathom Rajabhat University.

References

[1] X. Pingbo, F. Zhiyuan, F. Saifei, L. Hai, L. Chun, Y. Guanpeng, C. Qingmin, Z. Yanyan, Z. Fanming, Study on the sensitization of Gd^{3+} on Ce^{3+}/Tb^{3+} co-doped GBS scintillating glass, J. Non-Cryst. Solids. 481 (2018) 441 – 446.

[2] Z. Jingtao, L. Huang, L. Tianyu, Z. Shilong, X. Shiqing, Luminescent properties of Eu^{3+} doped heavy tellurite scintillating glasses, J. Lumin. 205 (2019) 342 – 345.

[3] Y. Takayuki, U. Jumpei M. Hirokazu, F. Yutaka, T. Setsuhisa, Optical and scintillation properties of Ce-doped $34Li_2O$-5MgO-$10Al_2O_3$-$51SiO_2$ glass, J. Non-Cryst. Solids. 431 (2016) 140 – 144.

[4] K. Preet, S. Devinder, S. Tejbir. Gamma rays shielding and sensing application of some rare earth doped lead-alumino-phosphate glasses, Radiat. Phys. Chem. 144 (2018) 336 – 343.

[5] L. Shamshad, G. Rooh, P. Limkitjaroenporn, N. Srisittipokakun, W. Chaiphaksa, H.J. Kim, J. Kaewkhao, A comparative study of gadolinium based oxide and oxyfluoride glasses as low energy radiation shielding materials, Prog. nucl. Energy. 97 (2017) 53 – 59.

[6] C. Eevon, M.K. Halimah, A. Zakaria, C.A.C. Azurahanim, M.N. Azlan, M.F. Fazn, Linear and nonlinear optical properties of Gd^{3+} doped zinc borotellurite glasses for all-optical switching applications, Results Phys. 6 (2016) 761 – 766.

[7] S. Kaewjang, U. Maghanemi, S. Kothan, H.J. Kim, P. Limkitjaroenporn, J. Kaewkh, New gadolinium based glasses for gamma-rays shielding materials, Nucl. Eng. Des. 280 (2014) 21 – 26.

[8] A.M.S. Issa, K. Ashok, M.I. Sayyed, M.G. Dong, Y. Elmahroug, Mechanical and gamma-ray shielding properties of TeO_2-ZnO-NiO glasses, Mater. Chem. Phys. 212 (2018) 12 – 20.

[9] N. Chanthima, J. Kaewkhao, Investigation on radiation shielding parameters of bismuth

borosilicate glass from 1 keV to 100 GeV, Ann. Nucl. Energy 55 (2013) 23 – 28.
[10] R. Laopaiboon, J. Laopaiboon, S. Pencharee, S. Nontachat, C. Bootjomchai, The effects of gamma irradiation on the elastic properties of soda lime glass doped with cerium oxide, J. Alloys Compd. 666 (2016) 292 – 300.
[11] M.I. Sayyed, Bismuth modified shielding properties of zinc boro-tellurite glasses, J. Alloys Compd. 688 (2016) 111 – 117.
[12] M.Ç. Ersundu, A.E. Ersundu, M.I. Sayyed, G. Lakshminarayana, S. Aydin, Evaluation of physical, structural properties and shielding parameters for K_2O-WO_3-TeO_2 glasses for gamma ray shielding applications, J. Alloys Compd. 714 (2017) 278 – 286.